PHYSICAL REVIEW B VOLUME 15, NUMBER 10 15 MAY 1977

Hydrogen locations and motions in the metallic-hydride system Ta_6SH_x. I. Temperature dependence of the proton NMR linewidth and second moment*

Y. S. Hwang, D. R. Torgeson, and A. S. Khan
Department of Physics and Chemistry, Ames Laboratory–ERDA, Iowa State University, Ames, Iowa 50011

R. G. Barnes
Physikalische Chemie III, Technische Hochschule, D-6100 Darmstadt, Federal Republic of Germany and Ames Laboratory–ERDA and Department of Physics, Iowa State University, Ames, Iowa 50011

(Received 17 December 1976)

Proton magnetic-resonance measurements in the metallic-hydride system Ta_6SH_x are reported, covering the temperature range 4.2–380 K and the frequency range 2.4–51 MHz, with hydrogen concentrations in the range $0.79 \leq x \leq 1.40$. The measured second moments, at 4.2 K, lie between 6.1 and 7.0 Oe^2 and vary slightly with hydrogen concentration. Second-moment calculations show that the dipolar contribution from tantalum is mainly responsible for the observed linewidth. Comparison of experimental and calculated results indicates several sets of interstitial sites appropriate for the location of the hydrogen. Line narrowing of the resonances occurs in two stages characterized by the average activation energies, $E_{act} = 0.01$ eV for $4.2 < T \leq 140$ K, and $E_{act} = 0.1$ eV for $140 \leq T \leq 300$ K, respectively, and corresponding to localized and long-range motional processes. At higher temperatures the line narrowing is limited by inhomogeneous broadening due to the bulk paramagnetism of the material. Room-temperature measurements of the magnetic-field dependence of the linewidth for $Ta_6SH_{1.40}$ yield a susceptibility of 1.6×10^{-6} g^{-1}, in agreement with the directly measured value. Knight shifts are small ($\sim 10^{-3}$%) in all samples, and in combination with the measured susceptibility suggest a nearly fully ionized hydrogen atom, or proton state.

I. INTRODUCTION

The group-V*b* metal-hydrogen systems have been the subject of a wide range of experimental investigations in recent years. These studies have been motivated in large part by the significance of the metals vanadium, niobium, and tantalum to both fission and fusion reactor technology as well as to the design and construction of superconducting cavities and energy storage devices. More recently, interest in transition-metal hydrides, especially hydrides of intermetallic compounds, as hydrogen-storing materials has brought additional impetus to their study.

The metallic compound Ta_6S, which belongs to the class of metal-rich sulfides that also includes such examples as $Nb_{21}S_8$ and V_3S, dissolves hydrogen exothermally at temperatures in the range 300–550 °C to form the hydride system, Ta_6SH_x, with $x \lesssim 2$.[1] In Ref. 1, the standard entropy of dissolved hydrogen was observed to be similar to that in the parent metal, tantalum. On the other hand, the crystal structure of Ta_6S is rather different from those of the transition metals and their typical binary-alloy systems.[2] With such a high metal-sulfur ratio, the question arises as to how significantly the hydrogen behavior is affected by the presence of the sulfur. Identification of hydrogen-sulfur interaction might aid in understanding hydrogen-oxygen interactions in the group-V*b* metals which pose a situation of greater practical relevance.

The subject of NMR studies of transition-metal hydrides was reviewed recently by Cotts.[3] Although many such investigations have dealt with binary hydride systems, only a few have concerned ternary systems.[4-6] In the present work, two distinct line-narrowing processes are observed in the temperature dependence of the proton resonance linewidth. One of these can be clearly identified as the long-range translational diffusion observed in other hydrides.[3] The second process is evident at much lower temperatures (10–50 K) and appears to originate from localized motion of the hydrogen within some "cage" framework. In addition to determining the hydrogen self-diffusion parameters from the temperature dependence of the proton resonance linewidth, an attempt has been made to deduce the probable locations of the hydrogen in the Ta_6S structure from the second moments of the spectra at 4.2 K and to elucidate the most probable diffusion paths at higher temperatures. The small values of the proton Knight shifts and the high susceptibility of the hydrides, revealed by strong inhomogeneous line broadening at high temperatures, furnish a basis for concluding that the hydrogen is essentially completely ionized to H^+ in this system.

II. EXPERIMENTAL DETAILS

A. Sample preparation and analysis

Powdered tantalum metal (99.99%) was obtained by thermal decomposition of tantalum hydride under a continuous vacuum at temperatures in the range 850–900 °C, the hydride having been previously synthesized by hydriding tantalum chips. The compound Ta_6S was prepared in two steps; first weighed amounts of Ta metal and sulfur were heated to temperatures between 700 and 800 °C in an evacuated Vycor tube for several days. Secondly, the samples were inductively heated to about 1300 °C for 3 h in a tungsten crucible, and then slowly cooled to room temperature. Samples were characterized by metallography and Guinier x-ray powder patterns. These techniques did not show the presence of any contaminating phases.

The samples of Ta_6S were hydrided in a conventional gas volumetric apparatus and this has been described previously.[1] The Ta_6S was outgassed at temperatures in the range 850–900 °C for several hours and a measured amount of hydrogen from thermal decomposition of uranium hydride was introduced into the system and the sample was slowly cooled to about 300 °C and left overnight, before cooling to room temperature.[1] The hydrogen content was established by a hot vacuum extraction technique.[7]

B. NMR instrumentation

The NMR measurements were made with induction spectrometers[8] employing crystal-stabilized radio-frequency sources and Varian Associate V4230B crossed-coil probes. Conventional 400-channel nuclear analyzers adapted for NMR were used for signal averaging.[9] Resonance data were obtained at nominal frequencies between 2.4 and 51 MHz, corresponding to magnetic field strengths of 500 Oe and 12 kOe, respectively, to check the dependence upon applied field strength. However, most of the spectra were accumulated at a nominal frequency of 28 MHz. Signal-averaging periods of 30 to 180 min were required for good spectral resolution for the several samples with the accumulation period dependent upon hydrogen concentration and sample temperature.

Spectra were measured at liquid-helium and liquid-nitrogen bath temperature and at other temperatures a gas-flow cryostat system[10] was employed. Controlled boiling of liquid helium provided the source of cold gas for maintaining sample temperatures in the range 20–90 K. For the range 90 K to room temperature, liquid nitrogen was boiled at a controlled rate. Temperature above room temperature were attained by flowing heated nitrogen gas over the sample at a steady rate.

When using the gas-flow technique, a small temperature gradient (less than 4 °C) did exist across the sample. To reduce this gradient, the gas-flow rate was maximized whenever possible and the sample lengths were minimized consistent with obtaining reasonable NMR signal-to-noise ratios. Temperatures were monitored using thermocouples either in the sample or as near to the sample as possible consistent with minimum noise injection into the spectrometer via the thermocouple leads.

III. EXPERIMENTAL RESULTS

Proton-magnetic-resonance spectra in Ta_6SH_x were measured in the temperature range 4.2–380 K and frequency range 2.4–51 MHz for $x = 0.79$, 0.87, 1.2, and 1.4. Within this composition range, all Ta_6SH_x form solid solutions for $T \geq 300$ K.[1] In addition, x-ray powder patterns at 90 K show that $Ta_6SH_{1.40}$ has the same structure as Ta_6S at 300 K, indicating no precipitation of other phases. The variation of the measured peak-to-peak separation of the absorption derivative signal at 28 MHz as a function of temperature is shown in Figs. 1(a) and 1(b) for the $x = 0.79$ and 1.2 compositions. Several characteristic features are to be noted: (i) the narrowing process has two clearly discernible stages, a break between the two occurring at approximately 140 K. (ii) The motional narrowing process is already evident at $T \sim 20$ K, which is most unusual for metallic hydride systems.[3] (iii) The rigid-lattice linewidth at 4.2 K decreases with decreasing hydrogen content. (iv) At high temperatures ($T \geq 300$ K), the linewidth remains constant and is independent of the temperature. However, the linewidths in this region are field dependent, as will be discussed further below.

At 4.2 K the $x = 1.2$ and $x = 1.4$ samples show good Gaussian line shapes, whereas for $x = 0.79$ and 0.87, the shape may be described as close to Gaussian. At higher temperatures, in the motionally narrowed regime, the shape is Lorentzian for all compositions.

A. Rigid-lattice second moments

The experimental second moments of the four samples at 4.2 K were obtained by direct numerical integration of the recorded derivative traces. The second moment for each sample was taken as the average of the values for up- and downfield scan directions. Fitting the function,[11] $f(H - H_0) = A \exp(-b|H - H_0|^n)$, where n is permitted to vary between 1.5 and 4.0, to the derivative

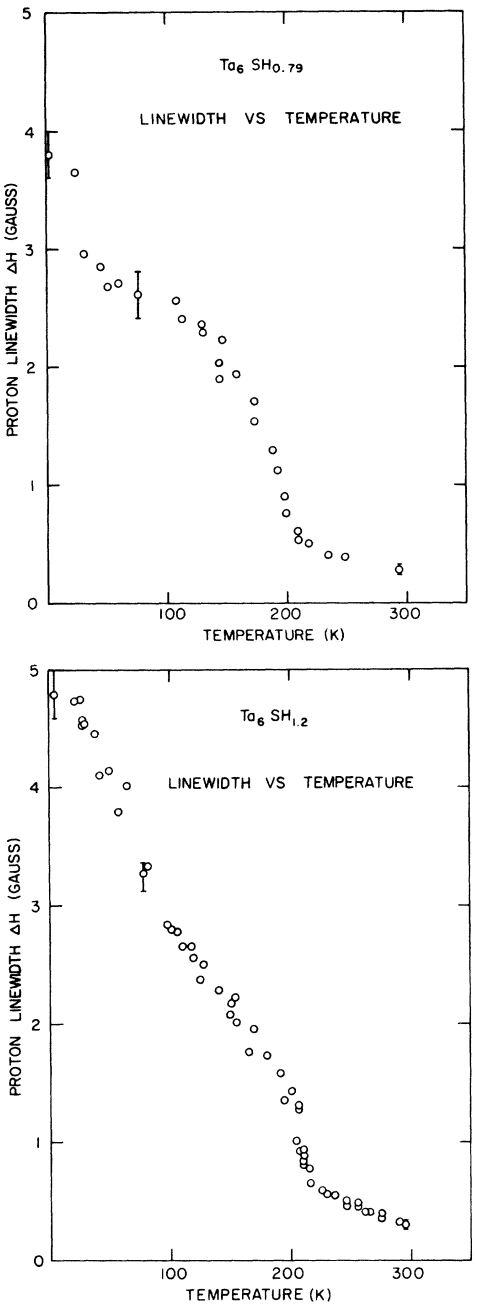

FIG. 1. Temperature dependence of the proton resonance linewidth in Ta_6SH_x at 28 MHz. (a) $x=0.79$, (b) $x=1.2$.

traces was also done. It was found that this method yielded values differing by as much as 15% when the derivative could not be fit by a single n value due to slight asymmetry of the trace. For a good Gaussian, the difference between the two methods (direct integration and shape-function fitting) was less than 2%. The final best measurements of the second moments and linewidths at 4.2 K are summarized in Table I.

As remarked above, for $T \geq 300$ K, the linewidth is field dependent, indicative of inhomogeneous broadening. In Fig. 2 is shown the field dependence of the linewidth at 300 K for three of the samples. The intercepts of 0.08 and 0.11 Oe in Fig. 2 correspond to the motionally narrowed intrinsic linewidth at 300 K. Drain has estimated that for a close-packed powder,[12] the volume susceptibility can be determined from the slope of the linewidth vs operating frequency (or field) plot. The susceptibility obtained from Fig. 2 is then 1.61×10^{-6} g^{-1} for $x=1.4$, in good agreement with the directly measured value of 1.36×10^{-6} g^{-1}. The linewidths at 300 K and 28 MHz obey the relation $\Delta H = 0.05 + k\chi_V$ with $k = 2.2\times10^4$ G cm^3. The intercept value of 0.05 Oe is in excellent agreement with the measured magnetic field inhomogeneity of the electromagnet of 0.048 ± 0.008 Oe at 28 MHz.

Since the broadening at 300 K is homogeneous, the T_2 determined from spin-echo Carr-Purcell-Meiboom-Gill echo-envelope measurements should continue to increase with temperature due to the hydrogen diffusion, whereas the linewidth remains constant. This behavior of T_2 has been observed[13] for the samples $x=0.87$, 1.2, and 1.4 in the temperature range $300 \leq T \leq 360$ K, and will be reported elsewhere.

B. Analysis of line-narrowing behavior

The strikingly novel feature of the experimental observations, as seen clearly in Figs. 1(a) and 1(b), is the appearance of motional narrowing of the linewidth already in the vicinity of 20 K. Qualitatively, the impression is immediately gained that two motional-narrowing processes occur, one of which must have an unusually low activation energy. This is not characteristic of hydrogen-linewidth behavior in metal-hydride systems studied to date, as these typically show rigid-lattice behavior at temperatures below about 150 K.[3]

To analyze the data, we employ a formalism in-

TABLE I. Experimental second moments and linewidths of the proton resonance in Ta_6SH_x at 4.2 K.

Sample $x=$	Second moment (Oe^2)	Linewidth (Oe)
0.79	6.1 ± 0.7	3.8 ± 0.2
0.87	7.0 ± 0.3	4.0 ± 0.1
1.2	6.3 ± 0.6	4.8 ± 0.2
1.4	6.5 ± 0.2	4.8 ± 0.1

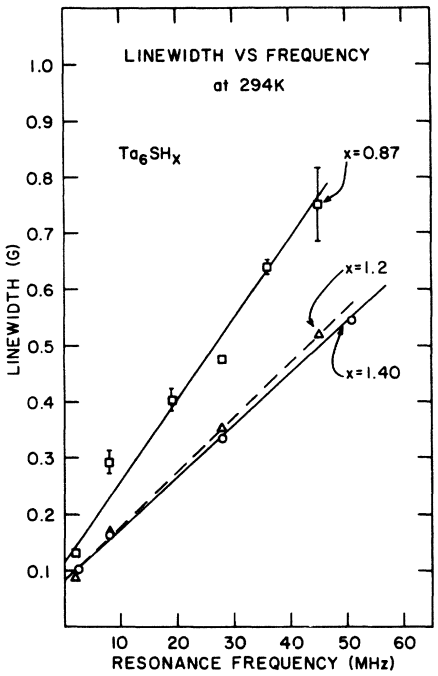

FIG. 2. Dependence of the proton resonance linewidth on resonance frequency in Ta_6SH_x samples.

troduced by Hendrickson and Bray[14] in their studies of similar two-stage narrowing behavior in alkali-metal glasses. The linewidth ΔH is related to an activation energy E_{act} and temperature T by the expression

$$\ln\left(\frac{1}{\Delta H}-\frac{1}{\Delta H_0}\right)=-\frac{E_{act}}{kT}+\ln\left(\frac{1}{B}-\frac{1}{\Delta H_0}\right), \qquad (1)$$

where ΔH_0 is the rigid-lattice linewidth and B is an assumed temperature-independent linewidth related to the spin-spin relaxation time of the excited (jumping) ionic species. Plots of this form of the linewidth data of the four samples studied are shown in Fig. 3. The plots reveal clearly the break into two straight-line segments which have approximately the same slopes for all four compositions. In determining E_{act} from Eq. (1), the magnetic inhomogeneous broadening, which varies for the different samples, has been subtracted from the ΔH and ΔH_0 values. A least-squares fit of the data to Eq. (1) then yields the E_{act} and B values, and these are listed in Table II.

The Hendrickson-Bray (HB) analysis contains no model-dependent assumptions as to the physical origin of the motional-narrowing process. Assuming that the high-temperature process is indeed normal translational diffusion as in other hydrides, then the usual Bloembergen-Pound-Purcell[15] (BPP) or Kubo-Tomita[16] analysis may be employed to obtain an activation energy and

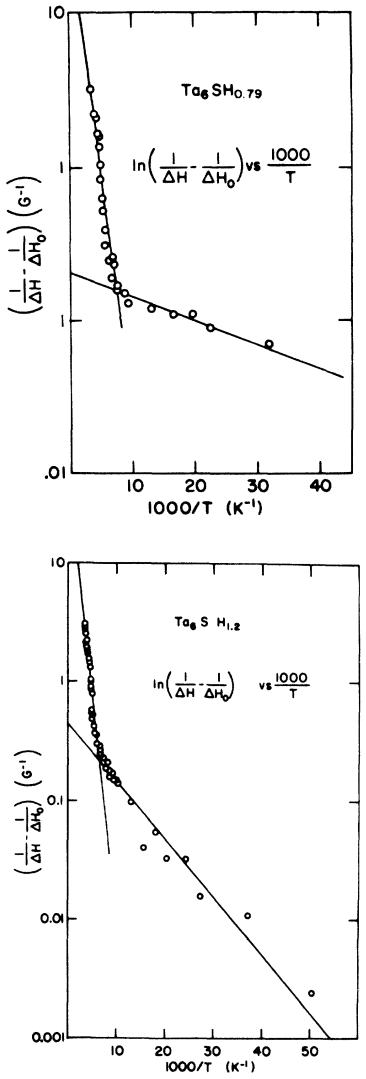

FIG. 3. Semilogarithmic dependence of the reciprocal of the proton linewidth in Ta_6SH_x on reciprocal temperature, in the manner of Hendrickson and Bray (Ref. 14). (a) $x=0.79$, (b) $x=1.2$.

attempt frequency. The dipolar correlation time τ_d is given in terms of the measured linewidth ΔH and rigid-lattice width ΔH_0 by

$$\tau_d=\frac{4\ln 2}{\gamma\pi}\,\frac{1}{\Delta H}\tan\left[\frac{\pi}{2}\left(\frac{\Delta H}{\Delta H_0}\right)^2\right], \qquad (2)$$

where γ is the gyromagnetic ratio of the proton. As in the HB analysis, the high-temperature residual linewidth has been subtracted from both ΔH and ΔH_0 before applying Eq. (2). Assuming, as is customary,[3] that

$$\tau_d=\tau_0\exp(E_{act}/kT), \qquad (3)$$

then E_{act} values are determined from the plot of

TABLE II. Values of the activation energy for hydrogen diffusion E_{act} determined from the two methods of analyzing the linewidth-vs-temperature data, as described in the text. The linewidth parameter B determined from the Hendrickson-Bray analysis is also listed.

Low-temperature region E_{act} (eV) HB analysis	B (Oe)	Sample x	High-temperature region E_{act} (eV) HB analysis	BPP analysis	B (Oe)
2.8×10^{-3}	2.03	0.79	0.083	0.07	5.4×10^{-3}
8.2×10^{-3}	1.61	0.87	0.09	0.07	5.1×10^{-3}
9.2×10^{-3}	1.37	1.2	0.14	0.12	3.0×10^{-4}
8.2×10^{-3}	1.18	1.4	0.12	0.11	8.6×10^{-4}

$\ln\tau_d$ vs $1/T$. The values of the activation energy so determined are also listed in Table II. The good agreement between the E_{act} values obtained from the two analyses supports the translational self-diffusion mechanism as being operative in the high-temperature region.

IV. DISCUSSION

A. Comparison of experimental and calculated rigid-lattice second moments

Since the line shapes at 4.2 K are essentially Gaussian for all four hydrogen concentrations studied, and since the linewidths appear to reach an upper limit at 4.2 K [as in Figs. 1(a) and 1(b)], it is reasonable to compare the experimental second moments at 4.2 K with theoretical expectations based on the Ta_6S structure and on a search for the most probable interstitial sites for the hydrogens in this structure.

X-ray diffraction spectra at 90 and 300 K show that Ta_6S crystallizes in the monoclinic space group $C2/c$ with unit cell parameters $a_0 = 14.16$ Å, $b_0 = 5.284$ Å, $c_0 = 14.79$ Å, and $\beta = 118.01°$.[2] The unit cell contains eight Ta_6S formula units. The structure is shown in plane view in Fig. 4 and can be regarded as consisting of chains of body-centered-pentagonal antiprisms of Ta atoms sharing faces in the b direction and interconnected via S atoms in the a and c directions. As seen in Fig. 4, each central Ta atom is surrounded by 12 other Ta atoms in a distorted icosahedron. The atomic coordinates in Ta_6S are listed in Table III.

There are 24 interstitial sites outside (between) the icosahedra and 120 within them which may be identified as reasonable locations for hydrogen occupation per unit cell. These interstitial sites are taken to be the centers of nearest-neighbor Ta tetrahedra, most of which are somewhat distorted. Positional parameters and the interstitial radii of these sites are categorized in Table IV. The Ta radius was taken as 1.32 Å in these calculations. Other secondary tetrahedral sites may be identified (total of 80) which are formed by three nearest-neighbor Ta atoms and one slightly more-distant Ta but these all have radii too small for them to be regarded as reasonable possibilities.

Nearest-neighbor tetrahedral sites contained entirely within the Ta icosahedra are of two types. The 40 type-1 sites (Nos. 13–17 in Table IV) are formed from two adjacent Ta on the central column (chain) and two adjacent Ta on one of the pentagonal rings. These sites occur in five sets of eight each and have Wyckoff designation (f). The 80 type-2 sites (Nos. 18–27 in Table IV) are formed from one Ta on the central chain, two adjacent Ta on the pentagonal ring above (below), and one Ta on the ring below (above). These occur in ten sets of eight each and also have Wyckoff designation (f). The type-1 sites are fairly regular tetrahedra, whereas the type-2 sites are distorted.

The tetrahedral sites which are between the Ta icosahedra may be coordinated with the sulfur atoms. As seen in Fig. 4, the S atoms may be regarded as running in zig-zag chains in the a direction, and these chains are cross linked in roughly the c direction. A tetrahedral site exists between each pair of S atoms, in both directions, for a total of 12 sites. In addition, there is another site at a distance $\frac{1}{2}b$ above or below each of these 12 sites, making a total of 24 tetrahedral sites between the Ta icosahedra. Each of these sites has a pair of S atoms coordinated with it, lying just outside the nearest-neighbor Ta tetrahedron. In Table IV, these sites are Nos. 1–6 and have Wyckoff designations (a), (b), (c), (d), (e), and (e), respectively.

One may also identify triangular sites in the region between the icosahedra. These are formed by two Ta atoms and one S atom, for a total of 48 sites, and are Nos. 7–12 in Table IV. With one exception, site No. 7, the radii of these triangular sites are too small. They may serve, however, as sites on the diffusive jump path of the hydrogen,

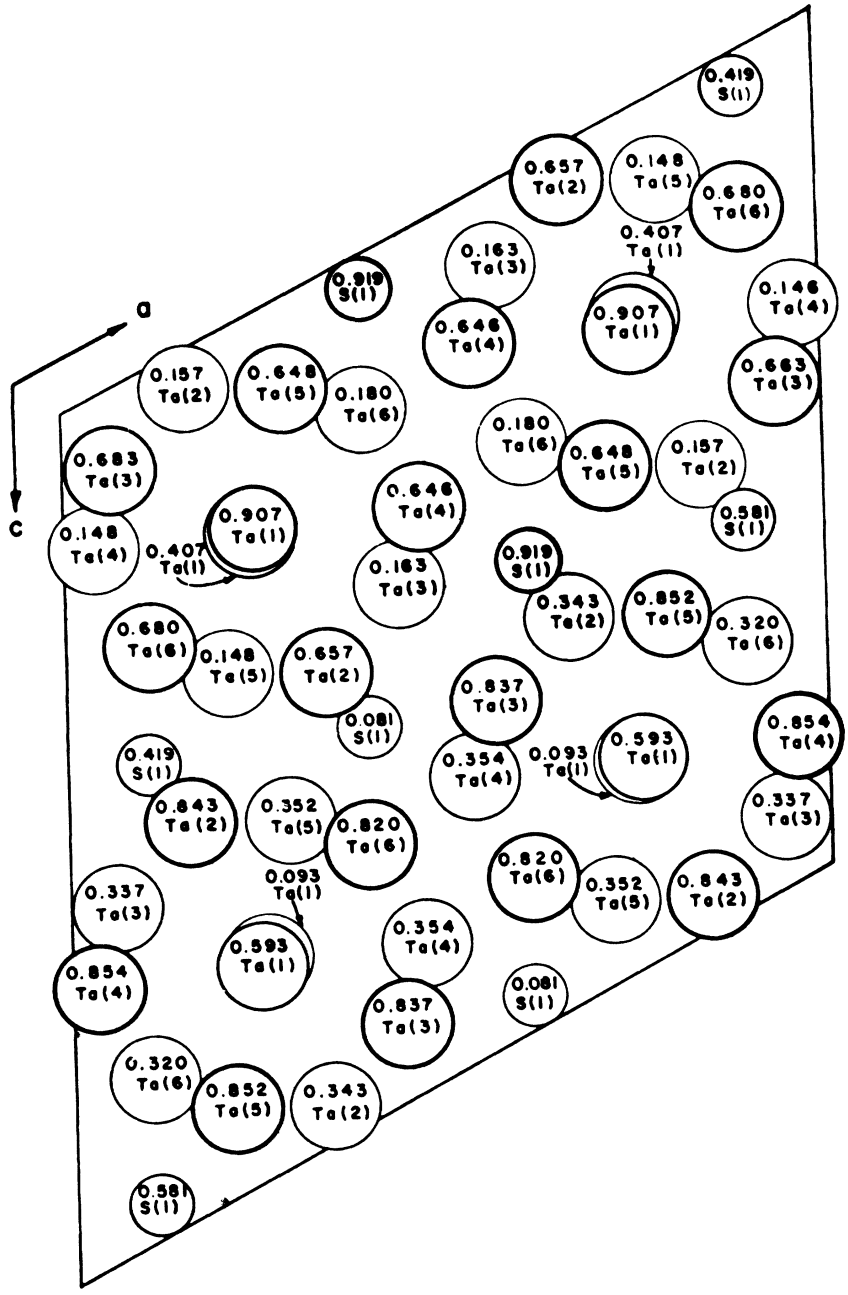

FIG. 4. Structure of Ta_6S as seen in projection on the *xz* plane.

as will be discussed further.

Finally, considered from the standpoint of the number of tetrahedral sites per Ta atom, the total of 144 nearest-neighbor sites per unit cell reduces to only three sites per Ta. This may be contrasted with the ratio of six tetrahedral sites per Ta in the *bcc* structure of Ta metal. Although the Ta-Ta separation of 2.64 Å along the central chain of the icosahedra in Ta_6S is substantially shorter than the nearest-neighbor separation in the metal (2.85 Å), other Ta-Ta separations in Ta_6S are somewhat greater (an average of 2.93 Å). Hence, the entire structure of Ta_6S is somewhat more open than that of Ta metal.

Since the linewidths level off at low temperature (as in Fig. 1), and the linewidths are Gaussian or close to Gaussian, the systems may reasonably be assumed to correspond to the rigid-lattice case at 4.2 K. Information concerning the possible sites occupied by the hydrogen can be derived from the second moments of the resonances at this temperature. The radii of the interstitial

sites tabulated in Table IV furnish an indication of the ability of the various sites to accommodate hydrogen. Consideration of negatively charged hydrogen ions can be excluded since the ionic radius is far too large to be accommodated in any of the sites. The possibility that neutral hydrogen is present also appears unlikely, and this point will be discussed further in Sec. IV C. Taking the radius of the positive hydrogen ion to be 0.44 Å, a value typical for metallic hydrides, the sites in Table IV(a) (except for Nos. 2 and 4), IV(c) and IV(d) appear to offer reasonable hydrogen locations. The triangular sites Nos. 8–12 have radii too small for them to be considered as probable hydrogen locations. However, as mentioned above, they offer good possible diffusive jump paths for the hydrogen.

The second moment of the proton resonance was calculated from the Van Vleck formula[17] appropriate to a powder, as generalized by Stalinski *et al.*,[18] to take account of the contributions from inequivalent sites to the total second moment. Following the notation of Weaver[19] and of Halstead,[4] the rigid-lattice second moment is given by

$$\langle \Delta H^2 \rangle = \left(C_I \sum_{i,j}^{N} \omega_i \alpha_i \alpha_j S_{ij} + C_S \sum_{i=1}^{N} \omega_i \alpha_i S'_{ij} \right) \Big/ \sum_k \omega_k \alpha_k , \qquad (4)$$

where $C_I = \frac{3}{5} \gamma_I^2 \hbar^2 \, I(I+1)$ and $C_S = \frac{4}{15} \gamma_S^2 \hbar^2 \, S(S+1)$ are, respectively, the constants for the like (^{1}H) and unlike (^{181}Ta) spin I and S; γ_I and γ_S are the magnetogyric ratios of ^{1}H and ^{181}Ta; ω_i is the relative number of i sites, α_i is the probability that an i site is occupied, and $S_{ij} = \sum_{j=1}^{N} r_{ij}^{-6}$ denotes the lattice sums with the origin taken at an i site and the summation extended over all j sites. Similarly, S'_{ij} denotes the lattice sum for the unlike spins. The major contribution to the second moment comes from the ^{181}Ta, the proton-proton contribution being less important, and the ^{33}S contribution being completely negligible.

The calculated second moments based on various combinations of hydrogen site occupancy are listed in Table V, and these should be compared with the experimental values listed in Table I. None of the results shown in Table V takes account of possible lattice expansion due to the hydrogen solution, which is typical of metal hydrides. In the case of $LaNi_5H_x$, for example, the volumetric expansion of $LaNi_5$ can be as large as 25% upon hydriding to $LaNi_5H_6$ although the crystal structure remains essentially unchanged.[20] This is an unusually large expansion, however. In the present case of Ta_6SH_x, our x-ray measurements provide two unusual results. First,

TABLE III. Atomic coordinates in the Ta_6S structure (from Ref. 2). Each position has eight equivalent positions in the unit cell.

Atom	Coordinates x	y	z
Ta(1)	0.25	0.41	0.25
Ta(2)	0.34	0.66	0.46
Ta(3)	0.44	0.16	0.41
Ta(4)	0.04	0.15	0.17
Ta(5)	0.21	0.15	0.40
Ta(6)	0.11	0.68	0.32
S(1)	0.39	0.92	0.04

TABLE IV. Characterization of interstitial sites in the Ta_6S structure. The atomic coordinates listed are representative. Coordinates of the remaining sites of each type are generated by the symmetry operations appropriate to the point symmetry of each site.

Assigned site No.	Coordinates x	y	z	Radius of interstitial site[a] (Å)
(a) Tetrahedral sites outside (between) the Ta icosahedra				
1	0.0	0.0	0.0	0.86
2	0.0	0.50	0.0	0.21
3	0.25	0.25	0.0	0.44
4	0.25	0.25	0.50	0.14
5	0.0	0.92	0.25	0.54
6	0.0	0.41	0.25	0.66
(b) Triangular sites outside (between) the Ta icosahedra				
7	0.46	0.64	0.01	0.49
8	0.50	0.58	0.10	...[b]
9	0.44	0.58	0.13	...
10	0.36	0.58	0.11	...
11	0.30	0.81	0.01	0.28
12	0.35	0.87	0.95	0.36
(c) Tetrahedral sites inside the Ta icosahedra (type 1)				
13	0.20	0.65	0.16	0.44
14	0.33	0.65	0.24	0.46
15	0.34	0.66	0.33	0.50
16	0.24	0.66	0.32	0.47
17	0.16	0.66	0.23	0.46
(d) Tetrahedral sites inside the Ta icosahedra (type 2)				
18	0.18	0.47	0.11	0.54
19	0.36	0.47	0.22	0.50
20	0.38	0.48	0.37	0.53
21	0.22	0.47	0.36	0.52
22	0.10	0.47	0.21	0.57
23	0.27	0.34	0.14	0.48
24	0.39	0.35	0.29	0.51
25	0.32	0.34	0.39	0.54
26	0.13	0.35	0.28	0.57
27	0.12	0.34	0.13	0.56

[a] Tantalum radius is taken to be 1.32 Å in Ta_6S.
[b] Site Nos. 8–10 have distance to nearest Ta $\leq$1.24 Å.

TABLE V. Calculated proton resonance second moments in Ta_6SH_x at 4.2 K, based on Eq. (4) of the text.

Trial structure	Combination of sites from Table IV	Hydrogen occupation	Location of hydrogen sites (inside or outside the icosahedra)	Second moment (Oe^2)
$A(1)$	3, 12	filled	outside	6.8
$A(2)$	1, 13	filled	inside and outside	6.7
$A(3)$	6, 16	filled	inside and outside	6.2
$A(4)$	18	filled	inside	
	24	half-filled, randomly	inside	6.4
$B(1)$	3, 15	filled	inside and outside	6.0
$B(2)$	6, 17	filled	inside and outside	7.1
$C(1)$	1, 2, 6	filled	outside	6.6
$C(2)$	1, 2, 3	filled	outside	6.4
$C(3)$	5, 6	filled		
	15	half-filled, randomly	inside and outside	6.8
$D(1)$	3, 5, 6	filled	outside	6.1
$D(2)$	1, 2, 5	filled	outside	7.0

the Ta_6S structure does not exhibit a measurable lattice expansion upon hydriding to $Ta_6SH_{1.40}$ at 300 K. Furthermore, $Ta_6SH_{1.40}$ x-ray powder patterns indicate no measurable lattice contraction between 300 and 90 K. These results are in contrast with TaH_x which exhibits both an expansion upon hydriding and a hydride contraction on cooling, with accompanying small changes in calculated second moments.

In Table V, entries A and C represent the results of the combinations of two and three inequivalent sites, respectively, which give second moment values in agreement with that observed in $Ta_6SH_{1.4}$ at 4.2 K within the experimental uncertainty. Entries B and D give, respectively, the extreme values of "unsuccessful" combinations of two and three inequivalent sites. Entry $A(1)$ is the only admissible calculated second moment for combinations of site Nos. 1–6 with site Nos. 7–12. Considering the small radii of site Nos. 8–12, this agreement may not be meaningful. Cases $C(1)$ and $C(2)$ involve combinations with site No. 2 which also has an unusually small radius, so that these cases may also be regarded as unreasonable.

When the experimental value of the rigid-lattice second moment for $Ta_6SH_{1.4}$ in Table I, 6.5 ± 0.2 G^2, is compared with entries A and C in Table IV, it is seen that several combinations of sites lead to acceptable second-moment values. Nevertheless, no combination of two sets of tetrahedral type-1 sites (inside the icosahedra) nor any combination of sites entirely outside the icosahedra yields a second moment in agreement with experiment. For example, the maximum second moment resulting from occupation of outside site Nos. 1, 3, 5, 6 alone is 5.4 (Oe^2). On the other hand, certain combinations of type-2 sites inside the icosahedra, or of type-1 or type-2 sites with sites outside the icosahedra, yield acceptable second moment values. It may be concluded that in $Ta_6SH_{1.4}$ at low temperatures (i.e., 4.2 K) the hydrogen occupies a combination of type-2 sites within the icosahedra or a combination of sites within and between the icosahedra.

B. Possible diffusion jump paths

Abrupt changes in the activation energy for hydrogen diffusion have been noted previously in certain composition ranges of the hydrides of scandium and yttrium.[21,22] However, the temperature ranges in which these changes occurred were much higher than in the present case, and the changes in E_{act} were of substantially smaller magnitude. In the present case, E_{act} changes by essentially an order of magnitude between the low- and high-temperature regions.

It is clear from Table II that in the high-temperature region E_{act} has a value in the range of those found in most binary-metal–hydrogen systems studied, further reinforcing the conclusion that the high-temperature motional process is translational diffusion of the hydrogen. The high-temperature E_{act} values are close to those obtained in TaH_x by Pedersen *et al.*,[23] Tanaka,[24] and Heidemann *et al.*[25] Tanaka[24] obtained $E_{act} = 0.144$ eV for $TaH_{0.1}$ in the temperature range $150 \leq T \leq 220$ K on the basis of proton line-narrowing measurements. Heidemann *et al.*,[25] using the Mössbauer

effect of ^{181}Ta, obtained $E_{act} = 0.14$ eV in the temperature range $225 \leq T \leq 400$ K for hydrogen concentrations in the range $0 \leq x \leq 0.17$. Pederson *et al.*,[23] on the basis of line-narrowing and T_1 measurements, obtained $E_{act} = 0.07$ eV in the α phase, 0.27 eV in the β_2 phase, and 0.13 eV in the β_1 phase. In the latter case, E_{act} was observed to decrease with increasing hydrogen content.

The nature of the motion in both low- and high-temperature regions merits some discussion. The analysis of Sec. III B furnishes evidence for long-range translational diffusion at high temperatures. As mentioned before, the x-ray powder pattern of $Ta_6SH_{1.4}$ at 90 K excludes the possibility of precipitation of other phases and the formation of SH^- ions. In addition, the NMR spectra show no evidence of a composite nature as would be expected if several different phases were present. All the evidence indicates that Ta_6SH_x remains single phase down to 4.2 K within the range of x values studied.

The two activated processes can be interpreted on the basis of the simple electrostatic model of Coogan and Gutowsky[26] if self-consistency among several parameters is assumed. Hydrogen diffusion has usually been analyzed in terms of motion between tetrahedral and octahedral sites in the *bcc* and *fcc* cubic lattices. Recently, the diffusion path through the intermediate triangular site has also been discussed.[27] In the Ta_6S structure, diffusion of the hydrogen from tetrahedral sites through the adjacent triangular sites to the nearest empty equivalent or inequivalent tetrahedral site appears to be responsible for the line narrowing of the proton resonance.

In applying Coogan and Gutowsky's electrostatic model, a screened interatomic Coulomb potential is employed.[26] Assume the hydrogen and tantalum are ionized with charges $Z_H e$ and $-Z_{Ta} e$, respectively, with the sulfur atoms carrying zero effective charge. This last assumption is not unreasonable.[28] The assumption of positively charged hydrogen ions is supported by the discussion in Sec. IV C, and negative hydrogen ions can be ruled out as mentioned previously. The energy at a tetrahedral (□) or triangular (△) site is then given by

$$E = Z_H^2 e^2 \left(\frac{Z_{Ta}}{Z_H} \sum_{Ta} \frac{e^{-Kr}}{r} + P \sum_{\substack{eq \\ sites}} \frac{e^{-Kr}}{r} + P' \sum_{\substack{ineq \\ sites}} \frac{e^{-Kr}}{r} \right), \quad (5)$$

where eq stands for equivalent, ineq stands for inequivalent, K^{-1} characterizes the screening length, and P and P' represent the probabilities of occupation of equivalent and inequivalent hydrogen sites, respectively. A typical value for K is 2×10^8 cm^{-1} for copper. If the diffusive jump is, say, from a type-2 □ site (e.g., No. 18 in Table IV) to the nearest empty inequivalent site [e.g., through the nearest △ site formed by Ta(1) with $y = 0.41$, Ta(2), and Ta(5)], then the activation energy is defined as the energy difference between the △ and □ sites.

Assuming that the jumps are uncorrelated, the calculated activation energies so obtained are summarized in Table VI. The screening constant has the value, $K = 1.1 \times 10^8$ cm^{-1} (somewhat smaller than usual), and the effective charges Z_H and Z_{Ta} have been varied over a range of plausible values. The summation in Eq. (5) was carried out to include all atoms within 5 Å of the site. To preserve charge neutrality, in the $Ta_6SH_{1.4}$ system, the magnitude of the charge on the hydrogen ion $Z_H e$ is in principle equal to $4.3 Z_{Ta} e$ without taking account of screening effects. The results in Table VI imply some slight screening and show a preference for a relatively high ionization of the hydrogen.

The hydrogen concentration in the γ phase of the TiH_x ($x = 2$) system, in which this model was originally applied with some success, is proportionately higher than that in the dilute $Ta_6SH_{1.4}$. Hence, the electrostatic proton-proton interaction is relatively much stronger in TiH_x than in $Ta_6SH_{1.4}$. This implies that for the latter system the first term in Eq. (5) dominates the other two terms.

The results in Table VI provide a qualitative picture of hydrogen ion motion at both low and high temperatures. Cases 1–3 in Table VI are concerned with the low-temperature localized motion inside the tantalum icosahedra; cases 4 and 5 concern low-temperature localized motion for sites 3 and 5 of Table IV; cases 6 and 7 concern motion at high temperatures between sites inside and outside the icosahedra. Finally, cases 8–10 concern motion at high temperatures among the outside sites only. For illustrative purposes, cases 1, 4, 6, and 8 will be discussed. Starting with motion at low temperatures, we have the following:

Case 1. Hydrogens are assumed to occupy fully site No. 18 of Table IV and half of the sites No. 24 randomly. This configuration yields a second moment of 6.4 Oe^2. The assumed diffusive jump path carries the hydrogen through the (△) site formed by Ta(1), Ta(2), and Ta(5) to its nearest empty inequivalent site (No. 23, Table IV), and for this Eq. (5) yields an activation energy of the same order as the low-temperature experimental value. Such a path can occur between type-1 (□) sites (case 3) or type-2 sites (case 1), or between type-1 and type-2 sites (case 2).

TABLE VI. Calculated activation energies for hydrogen diffusion for various possible jump paths, based on Eq. (5) in text. For all cases the screening constant, $K = 1.1 \times 10^8$ cm^{-1}. Values in parentheses show the effect of changes in the tantalum ion charge.

Case	Starting-point site (Table IV)	Configuration of saddle-point site	Activation energy (eV) for assumed ionic charges as follows: $Z_H = 0.9$		$Z_H = 0.8$		$Z_H = 0.7$	
			$Z_{Ta} = -0.18$	(-0.20)	$Z_{Ta} = -0.16$	(-0.18)	$Z_{Ta} = -0.14$	(-0.16)
1	18 ($y = 0.47$)	Ta(1), [a] (2), [b] (5)	0.013	(0.004)	0.010	(0.003)	0.008	(0.001)
2	18 ($y = 0.47$)	Ta(1), [a] (3), [c] (5)	0.039	(0.027)	0.031	(0.020)	0.024	(0.014)
3	13 ($y = 0.66$)	Ta(1), [a] (1), [d] (5)	0.011	(0.001)	0.009	(0.000)	0.007	(-0.001)
4	3 ($y = 0.25$)	Ta(5), (5), [e] S(1) [f]	0.011	(0.007)	0.009	(0.005)	0.007	(0.003)
5	5 ($y = 0.42$)	Ta(6), (4), [e] (4) [e]	0.015	(0.013)	0.012	(0.010)	0.009	(0.008)
6	5 ($y = 0.42$)	Ta(5), (4), [e] (6) [g]	0.20	(0.20)	0.16	(0.15)	0.12	(0.12)
7	14 ($y = 0.65$)	Ta(5), (4), [e] (6) [g]	0.063	(0.068)	0.050	(0.054)	0.038	(0.042)
8	5 ($y = 0.42$)	Ta(4), (4), [e] (5) [e]	0.08	(0.08)	0.06	(0.06)	0.05	(0.05)
9	5 ($y = 0.42$)	Ta(2), (6), [g] S(1) [h]	0.08	(0.10)	0.07	(0.08)	0.05	(0.06)
10	3 ($y = 0.25$)	Ta(4), (5), [e] S(1) [f]	0.19	(0.19)	0.15	(0.15)	0.11	(0.12)

[a] $y = 0.41$.
[b] $y = 0.16$.
[c] $y = 0.66$.
[d] $y = 0.91$.
[e] $y = 0.65$.
[f] $y = 0.92$.
[g] $y = 0.18$.
[h] $y = -0.08$.

Case 4. Hydrogens are assumed to occupy site Nos. 3 and 14 of Table IV, a configuration which also yields a second moment of 6.4 Oe^2. The assumed localized motion is a hopping motion in which for example the hydrogen in site No. 3 with y coordinate 0.25 jumps into the (△) site formed by S(1) and two Ta(5)'s and then jumps back. This type of localized motion can occur for sites outside the icosahedra (cases 4 and 5). Now we continue on to the motion at high temperatures.

Case 6. Hydrogens are assumed to occupy site Nos. 5 and 15. The assumed diffusive path carries the hydrogen from site No. 5 (outside the icosahedron) to a site (No. 14) inside the icosahedron through the (△) site formed by Ta(6), Ta(4), and Ta(5), resulting in an activation energy comparable to that of the high-temperature motional process.

Case 8. Hydrogens are assumed to occupy site Nos. 5 and 15. The diffusive path links site No. 5 ($y = 0.42$) to site No. 6 ($y = 0.91$) through the (△) site formed by two Ta(4)'s and one Ta(5). This again results in an activation energy of the same order as the high-temperature experimental value. Such zig-zag motion roughly parallel to the icosahedral chains possibly occurs between other sites outside the icosahedra as well.

Cases 9 and 10 describe motion roughly parallel to the xz plane among the sites outside the icosahedra. These cases also lead to activation energies comparable with that observed in the high-temperature motional narrowing region.

Based on this simple electrostatic model for the activation energy, it appears that at low temperatures the hydrogen either moves within the icosahedral cages or around the sites outside the icosahedra, partially reducing the dipolar interaction with the Ta nuclei. With increasing temperature, the hydrogens are able to jump into or out of the icosahedra and move freely through the lattice, reducing the dipolar interaction more completely.

The qualitative agreement between the activation energies listed in Table VI and the experimental values at low and high temperatures given in Table II can only be regarded as approximate in view of the extreme simplicity of the model and the complexities of the structure itself. Nonetheless, it furnishes a reasonable self-consistent picture for the hydrogen motion at all temperatures. Moreover, it suggests that the hydrogen

is nearly fully positively ionized, a conclusion further supported by the discussion in Sec. IV C.

C. Knight shift

The Knight shift, resulting from the contact hyperfine interaction between the nucleus and the conduction electrons of s character near the Fermi surface in the metal, may be written[29]

$$K_H = [Ia(s)/2\mu_I \mu_B]\chi_p M\xi , \quad (6)$$

where $a(s)$ is the hyperfine coupling constant, I is the nuclear spin, μ_I is the nuclear magnetic moment, μ_B is the Bohr magneton, χ_p is the average susceptibility per atom, M is the atomic mass, and $\xi = P_F/P_A$ where P_F is the probability density at the nucleus averaged over the conduction electrons near the Fermi level and P_A is the probability density at the nucleus in the free atom.

Most transition-metal hydrides exhibit bulk paramagnetism similar to that of the transition metals themselves. Determination of the susceptibility of the Ta_6SH_x samples by means of the proton NMR has been described in Sec. III A. Taking $a(s) = 0.04$ g^{-1} for hydrogen,[30] and $\chi_p = 1.6 \times 10^{-6}$ g^{-1} for $Ta_6SH_{1.4}$, where we assume that the susceptibility measured is due primarily to spin paramagnetism, one obtains from Eq. (6), $K_H = 4.54\xi\%$. Taking as an average value of the measured Knight shift, $K_H = 4.4 \times 10^{-3}\%$, then $\xi = 9.7 \times 10^{-4}$. This suggests that the hydrogen is nearly fully ionized. Lower concentrations of hydrogen lead to a decrease in ξ since the susceptibility then increases (see Fig. 2). Similar arguments have been advanced in respect to the LaH_x,[30] TiH_x,[18] and ZrH_x,[31] systems.

V. SUMMARY AND CONCLUSIONS

Wide-line proton-magnetic-resonance measurements over the temperature range $4.2 \leq T \leq 380$ K show that hydrogen motion in the system Ta_6SH_x ($0 \leq x \leq 1.4$) occurs in two stages characterized by the average activation energies, $E_{act} = 0.01$ eV for $4.2 < T \leq 140$ K and $E_{act} = 0.1$ eV for $140 \leq T \leq 300$ K, corresponding to localized and long-range motional processes, respectively.

The low-temperature second-moment measurements have been used as a basis for discussing the possible locations of the hydrogen in the Ta_6S lattice. Occupation solely of type-1 tetrahedral sites within the Ta icosahedra or of tetrahedral sites solely between the icosahedra appears not to occur. Probable sites are combinations of type-2 sites within the icosahedra and/or combinations of sites within and between them.

Hydrogen motion in both low- and high-temperature regions may be qualitatively accounted for in terms of an electrostatic model for the diffusive jump process. The most probable diffusive jump paths pass through triangular sites between the tetrahedral sites.

The very small proton Knight shift and high susceptibility of the hydride indicate that the hydrogen contributes its electron to the conduction band of the metal lattice.

ACKNOWLEDGMENTS

The authors thank T. Gould for experimental assistance in the early stages of this investigation and H. F. Franzen for several helpful discussions. The support of the Alexander von Humboldt Foundation and the hospitality of Professor A. Weiss of the Technische Hochschule Darmstadt are gratefully acknowledged by one of us (R. G. B.).

---

*Work performed for the U. S. ERDA under Contract No. W-7405-eng-82.

[1]H. F. Franzen, A. S. Khan, and D. T. Peterson, J. Solid State Chem. 17, 283 (1976).
[2]H. F. Franzen and J. G. Smegill, Acta Crystallogr. B 26, 125 (1970).
[3]R. M. Cotts, Ber. Buns. Ges. Phys. Chem. 76, 760 (1972).
[4]T. K. Halstead, J. Solid State Chem. 11, 114 (1974).
[5]E. F. Khodsov, V. K. Prokopenko, and A. I. Linnik, Fiz. Tverd. Tela 16, 243 (1974) [Sov. Phys.-Solid State 16, 157 (1974)].
[6]R. G. Barnes, W. C. Harper, S. O. Nelson, D. K. Thome, and D. R. Torgeson, J. Less Common Metals 49, 483 (1976).
[7]D. T. Peterson and V. G. Fattore, Anal. Chem. 34, 579 (1962).
[8]D. R. Torgeson, Rev. Sci. Instrum. 38, 612 (1967).
[9]Conversion of the analyzer consists of the addition of a voltage-to-frequency converter for the incoming data and the addition of a crystal-controller time-base generator to advance the channel address in multiscalar mode. A linear amplifier interfaces the channel address voltage with the magnet, see D. R. Torgeson, Rev. Sci. Instrum. 44, 982 (1973).
[10]K. P. Roenker, Ph.D. dissertation (Iowa State University, 1973) (unpublished).
[11]W. C. Harper and R. G. Barnes, J. Magn. Res. 21, 507 (1976).
[12]L. E. Drain, Proc. Phys. Soc. Lond. 80, 1380 (1962).
[13]P. A. Hornung (private communication).
[14]J. R. Hendrickson and P. J. Bray, J. Magn. Res. 9, 341 (1973).
[15]N. Bloembergen, E. M. Purcell, and R. V. Pound,

Phys. Rev. 73, 679 (1948).
[16]R. Kubo and K. Tomita, J. Phys. Soc. Jpn. 9, 888 (1954).
[17]J. H. Van Vleck, Phys. Rev. 74, 1168 (1948).
[18]B. Stalinski, C. K. Coogan, and H. S. Gutowsky, J. Chem. Phys. 34, 1191 (1961).
[19]H. T. Weaver, J. Chem. Phys. 56, 3193 (1972).
[20]J. H. Wernick and S. Geller, Acta Crystallogr. 12, 662 (1959).
[21]H. T. Weaver, Phys. Rev. B 5, 1663 (1972).
[22]H. T. Weaver, Phys. Rev. B 6, 2544 (1972).
[23]B. Pedersen. T. Krogdahl, and O. E. Stokkeland, J. Chem. Phys. 42, 72 (1965).
[24]K. Tanaka and T. Hashimoto, J. Phys. Soc. Jpn. 34, 379 (1973).
[25]A. Heidemann, G. Kaindl, D. Salomon, H. Wipf, and G. Wortmann, Phys. Rev. Lett. 36, 213 (1976).
[26]C. K. Coogan and H. S. Gutowsky, J. Chem. Phys. 36, 110 (1962).
[27]S. A. Steward, Solid State Commun. 17, 75 (1975).
[28]H. F. Franzen, M. X. Umana, J. R. McCreary, and R. J. Thorn, J. Solid State Chem. 18, 1 (1976).
[29]W. D. Knight, Solid State Phys. 2, 93 (1956).
[30]D. S. Schreiber and R. M. Cotts, Phys. Rev. 131, 1118 (1963).
[31]S. L. Martin and A. L. G. Rees, Trans. Faraday Soc. 50, 343 (1954).